

Graphical Test for Discrete Uniformity and its Applications in Goodness of Fit Evaluation and Multiple Sample Comparison

Teemu Säilynoja^{1*}, Paul-Christian Bürkner², Aki Vehtari¹

¹ Department of Computer Science, Aalto University, Finland

² Cluster of Excellence SimTech, University of Stuttgart, Germany

* Corresponding author, Email: teemu.sailynoja@aalto.fi

Abstract

Assessing goodness of fit to a given distribution plays an important role in computational statistics. The *Probability integral transformation* (PIT) can be used to convert the question of whether a given sample originates from a reference distribution into a problem of testing for uniformity. We present new simulation and optimization based methods to obtain simultaneous confidence bands for the whole *empirical cumulative distribution function* (ECDF) of the PIT values under the assumption of uniformity. Simultaneous confidence bands correspond to such confidence intervals at each point that jointly satisfy a desired coverage. These methods can also be applied in cases where the reference distribution is represented only by a finite sample. The confidence bands provide an intuitive ECDF-based graphical test for uniformity, which also provides useful information on the quality of the discrepancy. We further extend the simulation and optimization methods to determine simultaneous confidence bands for testing whether multiple samples come from the same underlying distribution. This multiple sample comparison test is especially useful in Markov chain Monte Carlo convergence diagnostics. We provide numerical experiments to assess the properties of the tests using both simulated and real world data and give recommendations on their practical application in computational statistics workflows.

1 Introduction

Tests for uniformity play an essential role in computational statistics when estimating goodness of fit to a given distribution (Marhuenda, Morales, and Pardo 2005). This is because, even when the distribution of interest is not uniform, there are methods to reduce the problem into testing for uniformity by transforming a sample from the given distribution to a (discrete or continuous) uniform distribution.

1.1 Probability integral transformation

Transforming sampled values to a uniform distribution is usually achieved via the *probability integral transform* (PIT), provided the distribution of interest has a tractable *cumulative distribution function* (CDF) (D’Agostino and Stephens 1986). Let $y_1, \dots, y_N \sim g(y)$ be a sample from an unknown *continuous* distribution with *probability density function* (PDF) g . We want to know whether $g = p$, where p is the PDF of a known distribution with a tractable CDF. The PIT of the sampled value y_i with respect to p is

$$u_i = \int_{-\infty}^{y_i} p(y) dy. \quad (1)$$

If $g = p$, the transformed values u_i are continuously uniformly distributed on the unit interval $[0, 1]$, reducing the evaluation of the hypothesis into testing for uniformity of the transformed sample u_1, \dots, u_N . If the integral (1) does not have closed form, the CDF (and hence the PIT values) can still be computed with sufficient accuracy through numerical integration (e.g., quadrature), if at least the corresponding PDF is tractable.

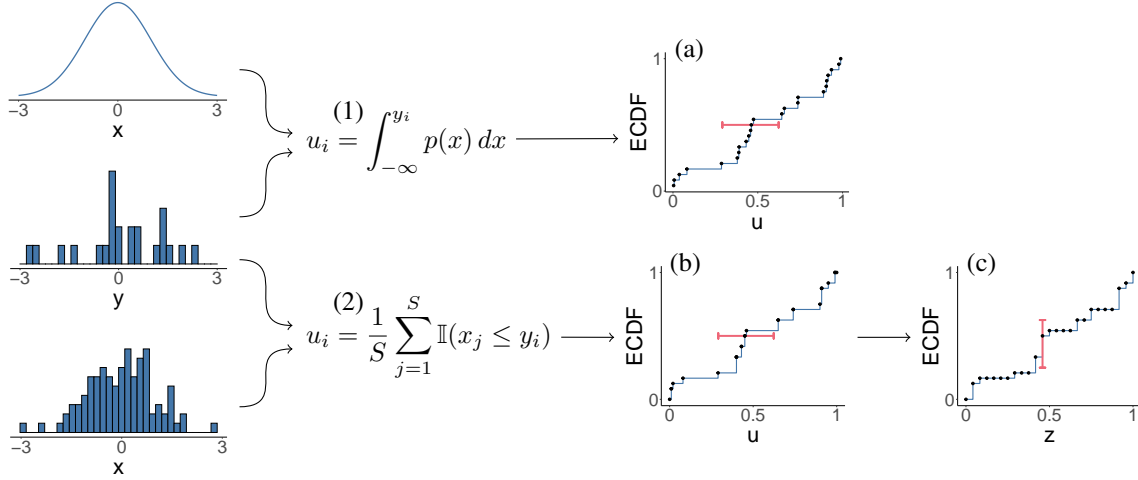


Figure 1: Given $y_1, \dots, y_N \sim g(y)$, and a distribution $p(x)$, the hypothesis $g = p$ can be assessed in two ways. (1) If the ECDF or the PDF of p has a closed form, the PIT values u_i are continuous and, if $g = p$, uniformly distributed. (a) The pointwise confidence intervals (red bars) for the ordered statistic $u_{(i)}$ are beta distributed and the simultaneous confidence intervals for the ECDF of u_i are given by Aldor-Noiman et al. (2013). (2) If a sample $x_1, \dots, x_S \sim p(x)$ can be obtained, the empirical PIT values u_i are discrete and, given $g = p$, uniformly distributed. (b) The pointwise confidence intervals of the discrete ordered statistic $u_{(i)}$ could be solved from Eq. (3). (c) The pointwise confidence intervals of the value of the ECDF of u_i at $z_i \in [0, 1]$ are binomially distributed and the simultaneous confidence intervals are obtained by the method presented in this paper.

If neither the CDF nor the PDF have closed form, but a comparison sample $x_1, \dots, x_S \sim p(x)$ can be drawn, the hypothesis $g = p$ can be evaluated through the empirical PIT values

$$u_i = \frac{1}{S} \sum_{j=1}^S \mathbb{I}(x_j \leq y_i), \quad (2)$$

where \mathbb{I} is the indicator function. Now, given $g = p$, the transformed values $u = u_1, \dots, u_N$ are distributed according to a discrete uniform distribution with $S + 1$ values $(0, 1/S, \dots, (S - 1)/S, 1)$. Accordingly, we can still apply uniformity tests to assess $g = p$, just that this time, we need to test for discrete uniformity.

Figure 1 shows an example of the *empirical cumulative distribution function* (ECDF) for u obtained through both Eq. (1) and Eq. (2). The figure also shows an example of a pointwise confidence interval for each ECDF. For the continuous integral of Eq. (1), the pointwise confidence interval can be computed from the continuous uniform ordered statistics distribution which is a common beta distribution. For the discrete sum of Eq. (2), the pointwise confidence interval can be computed from the discrete uniform ordered statistics distribution, with the cumulative distribution function of the i th ordered statistic $u_{(i)}$ given as

$$F_i(z) = \sum_{k=i}^N \binom{N}{k} z^k (1 - z)^{N-k}, \quad (3)$$

for $z \in (0, 1/S, \dots, (S - 1)/S, 1)$. The corresponding pointwise intervals do not have a nice form in general and, more importantly, the discrete ordered statistics do not exhibit Markovian structure (exploited by our new optimisation based approach) if there are possible ties in u (Arnold, Balakrishnan, and Nagaraja 2008, Ch. 3).

To make the computation of the simultaneous confidence bands more straightforward and efficient, we propose making an additional transformation by computing the ECDF of u at chosen evaluation points z_i :

$$F(z_i) = \frac{1}{N} \sum_{j=1}^N \mathbb{I}(u_j \leq z_i), \quad (4)$$

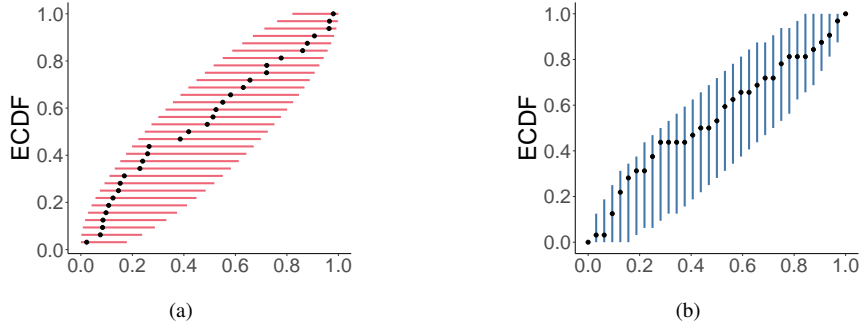


Figure 2: Simultaneous confidence bands: (a) Method by Aldor-Noiman et al.: Beta distribution-based 95% simultaneous confidence bands for quantiles are provided for reaching a set of ECDF values (along the x-axis). (b) Our method: For a set of evaluation quantiles, we provide binomial distribution-based 95% simultaneous confidence intervals for the ECDF value (along the y-axis).

where z_i are chosen as the ordered fractional ranks \tilde{r}_i of y_i , defined as

$$\tilde{r}_i = \frac{1}{N} \sum_{j=1}^N \mathbb{I}(y_j \leq y_i). \quad (5)$$

The ordered fractional ranks form a uniform partition of the unit interval independent of the distribution of y_i . Thus, they provide an ECDF that is easier to interpret than the corresponding ECDF based directly on the original sample y_i . The resulting ECDF is illustrated in Figure 1(c). As we will show, useful properties of this ECDF are that 1) its pointwise confidence intervals can be computed easily from the binomial distribution, with a quantile function already implemented in most widely used environments for statistical computing, and 2) the distribution of the ECDF trajectories is Markovian, which is exploited in Section 2.3.

1.2 Simultaneous confidence bands

The major challenge that arises when developing a uniformity test based on the ECDF is to obtain simultaneous confidence bands with the desired overall coverage. For this purpose, one needs to take into account the inter-dependency in the ECDF values and adjust the coverage parameter accordingly (we will discuss this in more detail in Section 2).

When considering whether a given ECDF could present a sample from a uniform distribution, we need to jointly consider all pointwise uncertainties. For a set of evaluation points $(z_i)_{i=1}^N$, we provide lower and upper confidence bands L_i and U_i respectively, that jointly satisfy

$$\Pr(L_i \leq F(z_i) \leq U_i \mid \forall i) = 1 - \alpha, \quad (6)$$

where $F(z_i)$ is the ECDF of a sample from either the standard uniform distribution or discrete uniform distribution on the unit interval evaluated at $z_i \in (0, 1)$ and $1 - \alpha$ is the desired simultaneous confidence level. In addition to offering a numerical test for uniformity, the simultaneous confidence bands provide an intuitive graphical representation of possible discrepancies from uniformity.

Aldor-Noiman et al. (2013) presented a simulation-based approach for computing simultaneous confidence band for the ECDF of the transformed sample acquired from Eq. (1) under the assumption of uniformity. In this paper, we present a simulation method inspired by Aldor-Noiman et al. (2013) as well as a new, faster optimization method for computing simultaneous confidence bands under uniformity, when the ECDF is computed from the empirical PIT values using Eqs. (2) and (4). Figure 2 contrasts the simultaneous confidence bands by Aldor-Noiman et al. (2013) against those obtained from our proposed method. Furthermore, we generalize our method and simultaneous confidence bands to test whether multiple samples originate from the same underlying distribution.

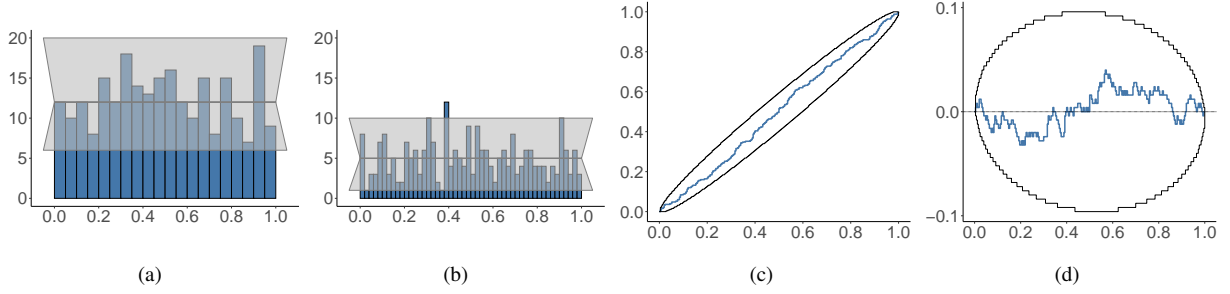


Figure 3: Four visualizations depicting the same random sample of 250 values. To assess uniformity of the sample, histograms (a) and (b) show a 95% confidence interval for each bin. Histograms can be sensitive to the number and placement of the bins selected, and the confidence intervals do not take into account possible inter-dependencies between the bin heights. For example, given the same sample, a 20 bin histogram stays within the confidence interval (a), but a 50 bin histogram exceeds the confidence interval (b). The ECDF plot (c) and ECDF difference plot (d) with 95% simultaneous confidence bands for the ECDF both show the sample staying within the given limits with the ECDF difference plot providing a more dynamic range for the visualization.

1.3 Related work

The idea of utilizing the ECDF to test uniformity is not new, but its potential has not yet been realized in full. For example, the well known Kolmogorov-Smirnov (KS) test, first introduced by Kolmogorov (see e.g. Massey Jr (1951), original article in Italian is Kolmogorov (1933)), is based on evaluating the maximum deviation of the sample ECDF from the theoretical CDF of the distribution to be tested against. Unfortunately, the KS test is relatively insensitive to deviations in the tails of the distribution (Aldor-Noiman et al. 2013), and numerous tests have been proposed to replace the KS test. An extensive comparison of more than thirty tests of uniformity of a single sample is provided by Marhuenda, Morales, and Pardo (2005).

Due to its ease of interpretation and familiarity to people even with basic statistical knowledge, a graphical method for assessing uniformity commonly used as part of many statistical workflows is plotting histograms. This can even be turned into a formal test of uniformity with confidence intervals for the individual bins (e.g., Talts et al. 2020). Drawbacks of histograms are that binning discards information, there can be binning artifacts depending on the choice of bin width and placement, and they ignore the dependency between bins. The proposed ECDF-based method doesn't require binning or smoothing, provides intuitive visual interpretation, and works for continuous Eq. (1) and discrete Eq. (2) values. An illustration and comparison of histograms with two binning choices and our new method is given in Figure 3. The visual range between the simultaneous confidence bands for the ECDF is often narrow when visualizing a sample with a large number of observations. Thus, to achieve a more dynamic range for the visualization, we recommend to show ECDF difference plots, instead, as illustrated in Figure 3(d). The ECDF difference plot is obtained by subtracting the values of the expected theoretical CDF (i.e., the identity function in $[0,1]$ in case of standard uniformity) from the observed ECDF values.

1.4 Summary of contributions

In this article, we focus on use case examples arising from inference validation and Markov chain Monte Carlo (MCMC) convergence diagnostics as part of a Bayesian workflow (Gelman, Vehtari, et al. 2020), but our developed methods are applicable more generally. Our use cases can be divided into two main categories: a single sample test for uniformity, and a multiple sample comparison where the hypothesis is tested that the samples are drawn from the same underlying (potentially non-uniform) distribution. We discuss both cases in more detail below.

We offer a graphical test for uniformity by providing simultaneous confidence bands for one or more ECDF trajectories obtained through the empirical probability integral transformation. As our first contribution, we modify an existing ECDF-based approach proposed by Aldor-Noiman et al. (2013) to take into account the discreteness of the fractional rank-based PIT values. This forms the basis for our proposed single and multi-sample tests.

As our second contribution, we provide both a simulation and optimization method to determine the adjustment needed to achieve a desired simultaneous confidence level for the ECDF trajectory given the fractional rank-based PIT

values. In addition to presenting a simulation-based adjustment following the method of Aldor-Noiman et al. (2013), we introduce a new optimization method that is computationally considerably more efficient in determining the needed adjustment, especially when bands with high resolution are desired for a large sample size. Although our focus is on providing a test with an intuitive graphical representation, we show that our method performs competitively when compared to existing uniformity tests with state-of-the-art performance. We demonstrate the usefulness of this graphical test in context of simulation based calibration approach for assessing inference methods (Talts et al. 2020).

Finally, as our third contribution, we generalize the graphical test as well as both the simulation and the optimization method to evaluate the hypothesis that two or more samples are drawn from the same underlying distribution. We demonstrate the usefulness of this graphical test in MCMC convergence diagnostics, where the currently most common graphical tools for assessing convergence are trace plots of the individual sampled chains.

1.5 Outline of the paper

In Section 2, we first provide a simulation-based method to determine simultaneous confidence bands for the ECDF of a single uniform sample and then present new more efficient optimization-based method. In Section 3, we extend the test to multiple sample comparison, and follow a similar structure by offering both a simulation and an optimization-based methods. We continue in Section 4 with simulated and real-world examples illustrating the application of our proposed method, and end with a discussion in Section 5.

2 Simultaneous Confidence Bands for the Empirical Cumulative Distribution

We propose simulation and optimization based approaches to providing the ECDF of a uniform sample with $1 - \alpha$ level simultaneous confidence bands that are compatible with empirical PIT values, that is, confidence bands with a type-1-error rate of α . Our approach is similar to that presented by Aldor-Noiman et al. (2013) with one central distinction illustrated in Figure 2. The method by Aldor-Noiman et al. (2013) obtains simultaneous confidence bands for the evaluation quantiles with fixed ECDF values based on beta distributions, that is, it obtains confidence bands along the horizontal axis (Figure 2(a)). In contrast, our new method provides simultaneous confidence bands for the ECDF values at fixed evaluation quantiles based on binomial distributions, that is, it obtains confidence bands along the vertical axis (Figure 2(b)). In the limit, as the sample size approaches infinity, there is no practical difference between the methods. However, when the number of possible unique ranks is small, our proposed method behaves better for smallest and largest ranks, and consistently if the ranks are further binned.

2.1 Pointwise confidence bands

Determining the pointwise confidence interval for the ECDF value of a sample from the continuous uniform distribution at a given evaluation quantile $z_i \in (0, 1)$ is rather straightforward. By definition, given a sample $u = u_1, \dots, u_N$, the ECDF value is

$$F(z_i) = \frac{1}{N} \sum_{j=1}^N \mathbb{I}(u_j \leq z_i). \quad (7)$$

As the sampled values, $u_j \in (0, 1)$, are expected to be continuously uniformly distributed, $Pr(u_j \leq z_i) = z_i$ for each $j = 1, \dots, N$. Thus, the values resulting from scaling the ECDF with the sample size N are binomially distributed as

$$NF(z_i) \sim \text{Bin}(z_i, N). \quad (8)$$

If we instead expect u to be sampled from a discrete uniform distribution with S distinct equally spaced values, $s_j = j/S$, by choosing the partition points to form a subset of these category values, we again have $Pr(u_j \leq z_i) = z_i$ for $j = 1, \dots, N$, and the marginal distribution of the scaled ECDF follows Eq. (8). Therefore the methods introduced in 2.2 and 2.3 can be used to determine simultaneous confidence bands for both continuous and discrete uniform samples, allowing for testing uniformity of both the continuous PIT values of Eq. (1) and the discrete empirical PIT values in Eq. (2).

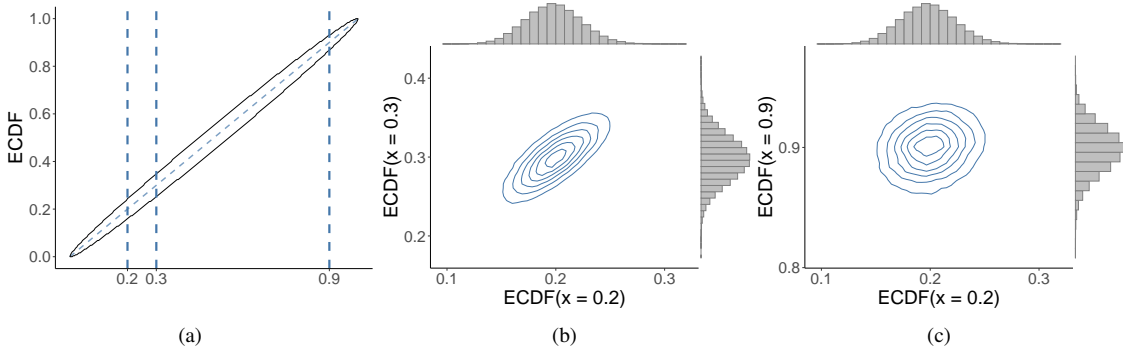


Figure 4: Dependence between the ECDF values of standard uniform samples evaluated at three distinct points. Simultaneous 95% confidence bands for the ECDF computed via either of the new methods introduced in this paper are shown in (a). In (b), one can see a stronger dependency between the ECDF values obtained at evaluation points close to each other whereas in (c) the ECDF values are only weakly dependent as the evaluation points far away from each other.

From Equation (8), it is straightforward to determine the $1 - \alpha$ level pointwise lower and upper confidence bands, L_i and U_i respectively, satisfying for all $i = 1, \dots, N$

$$\Pr(L_i \leq F(z_i) \leq U_i) = 1 - \alpha. \quad (9)$$

In contrast, determining the simultaneous confidence bands for ECDF trajectories (i.e., sets of ECDF values) is more complicated. In Figure 4, we illustrate the dependency between ECDF values at distinct evaluation quantiles, together with simultaneous confidence bands computed via either of the new methods described in the following sections. As is illustrated in the figure, ECDF values evaluated at two quantiles close to each other are strongly dependent while ECDF values evaluated at two quantiles far away from each other are only weakly dependent. In any case, these dependencies need to be taken into account when constructing simultaneous confidence bands.

2.2 Simultaneous confidence bands through simulation

Our goal is to define simultaneous confidence bands for the ECDF of a standard uniform distribution so that the interior of the confidence bands contains trajectories induced by that distribution with rate $1 - \alpha$, where $\alpha \in (0, 1)$.

In this section we describe a simulation based method for determining the simultaneous confidence bands for the ECDF trajectory. We follow steps similar to those introduced by Aldor-Noiman et al. (2013); with the exception that instead of determining limits for the Q-Q plot, we now determine the upper and lower limits of the ECDF values at the evaluation points z_i :

1. Choose a partition $(z_i)_{i=1}^K$ of the unit interval.
2. Determine coverage parameter γ to account for multiplicity in order to obtain the $1 - \alpha$ level simultaneous confidence bands:

$$\Pr(L_i(\gamma) \leq F(z_i) \leq U_i(\gamma) \mid \forall i = 1, \dots, K) = 1 - \alpha. \quad (10)$$

In determining these confidence bands, we use the knowledge from that the values of the scaled ECDF at each point z_i follow a binomial distribution and denote the value of the cumulative binomial distribution function with parameters N and z_i at $k \in \mathbb{N}$ by $\text{Bin}(k \mid N, z_i)$ and its inverse by $\text{Bin}^{-1}(q \mid N, z_i)$ for quantile $q \in [0, 1]$.

To find the desired coverage value γ , we simulate M draws from the standard uniform distribution. Let F^m denote the ECDF of the m th sample, $u_1^m, \dots, u_N^m \sim \text{uniform}(0, 1)$. For each sample, we find the largest value of γ such that the equal tail quantiles $L_i(\gamma) = \text{Bin}^{-1}(\frac{\gamma}{2} \mid N, z_i)$ and $U_i(\gamma) = \text{Bin}^{-1}(1 - \frac{\gamma}{2} \mid N, z_i)$ cover the sample ECDF, F^m ,

at each z_i . This value of γ for the m th sample is

$$\begin{aligned}
\gamma^m &= \arg \max_{\gamma} \{L_i(\gamma) \leq F^m(z_i) \leq U_i(\gamma) \mid \forall i\} \\
&= \arg \max_{\gamma} \left\{ \text{Bin}^{-1} \left(\frac{\gamma}{2} \mid N, z_i \right) \leq NF^m(z_i) \leq \text{Bin}^{-1} \left(1 - \frac{\gamma}{2} \mid N, z_i \right) \mid \forall i \right\} \\
&= \arg \max_{\gamma} \left\{ \frac{\gamma}{2} \leq \text{Bin}(NF^m(z_i) \mid N, z_i) \leq 1 - \frac{\gamma}{2} \mid \forall i \right\} \\
&= 2 \min_i \{ \min(\text{Bin}(NF^m(z_i) \mid N, z_i), 1 - \text{Bin}(NF^m(z_i) - 1 \mid N, z_i)) \}. \tag{11}
\end{aligned}$$

To obtain bands covering a $1 - \alpha$ fraction of the ECDFs of the simulated samples, we set γ to the α quantile of the values $\{\gamma^1, \dots, \gamma^M\}$. Since $\gamma^m > 0$ by construction, we also have $\gamma > 0$.

The following steps summarize the algorithm for simulating the adjusted coverage parameter γ and determining the $1 - \gamma$ level simultaneous confidence bands:

1. For $m = 1, \dots, M$:

- (a) Simulate $u_1^m, \dots, u_N^m \sim \text{uniform}(0, 1)$.
- (b) For $i = 1, \dots, K$, compute $F^m(z_i)$.
- (c) For $i = 1, \dots, K$, compute

$$\text{Bin}(NF^m(z_i) \mid N, z_i) \text{ and } \text{Bin}(NF^m(z_i) - 1 \mid N, z_i).$$

(d) Find the minimum probability

$$\gamma^m = 2 \min_i \{ \min(\text{Bin}(NF^m(z_i) \mid N, z_i), 1 - \text{Bin}(NF^m(z_i) - 1 \mid N, z_i)) \}.$$

2. Set γ to be the 100α percentile of $\{\gamma^1, \dots, \gamma^M\}$.

3. Form the confidence bands $[L_i(\gamma), U_i(\gamma)] = [\text{Bin}^{-1}(\frac{\gamma}{2} \mid N, z_i), \text{Bin}^{-1}(1 - \frac{\gamma}{2} \mid N, z_i)]$ for $i = 1, \dots, K$.

2.3 Simultaneous confidence bands through optimization

We propose also a computationally more efficient optimization based method for determining the simultaneous confidence bands. We denote the interior of the confidence bands for the ECDF at quantile z_i as $\tilde{I}_i(\gamma)$. By denoting $r_i = NF(z_i)$, the scaled interior $I_i(\gamma)$ for r_i is given by

$$I_i(\gamma) = \left\{ r \in \{0, \dots, N\} \mid \text{Bin}^{-1} \left(\frac{\gamma}{2} \mid N, z_i \right) \leq r \leq \text{Bin}^{-1} \left(1 - \frac{\gamma}{2} \mid N, z_i \right) \right\}. \tag{12}$$

As is common for discrete statistical tests, we treat the borders between interior and exterior as belonging to the interior. Based on $I_i(\gamma)$, we can easily obtain $\tilde{I}_i(\gamma)$ as $r \in I_i(\gamma)$ is equivalent to $r/N \in \tilde{I}_i(\gamma)$.

A scaled ECDF trajectory defined as

$$t_0^K = ((z_i)_{i=0}^K, (u_i)_{i=0}^K) \tag{13}$$

with $z_0 = 0$ and $z_K = 1$ stays within the simultaneous confidence bands completely if and only if $u_i \in I_i(\gamma)$ for all $i \in \{0, \dots, K\}$. If we denote the set of trajectories fulfilling $u_i \in I_i$ as T_i , we can write the set of trajectories which are completely within the simultaneous confidence bands as

$$T(\gamma) = \bigcap_{i=0}^K T_i(\gamma). \tag{14}$$

In order for the simultaneous confidence bands to have confidence level $1 - \alpha$, we must have

$$Pr(T(\gamma)) = 1 - \alpha. \tag{15}$$

Due to the pairwise independence of the original draws u_i (by assumption), the distribution of the ECDF trajectories is Markovian. That is, any ECDF trajectory t_{i+1}^K beyond a given point $(z_i, F(z_i))$ only depends on $(z_i, F(z_i))$ and not

on the values the ECDF takes at points before z_i . This implies that, under uniformity of the original distribution, the ECDF trajectory beyond $(z_i, F(z_i))$ is equivalent to the ECDF trajectory of a uniform distribution over the interval $[z_i, 1]$ shifted upwards by $F(z_i)$. For the implied scaled ECDF trajectory t_{i+1}^K beyond $(z_i, r_i = NF(z_i))$ this means that the growth $r_{i+1} - r_i$ of the ECDF from z_i to z_{i+1} is binomially distributed with $N - r_i$ trials and success probability

$$\tilde{z}_{i+1} = \frac{z_{i+1} - z_i}{1 - z_i}, \quad (16)$$

and so we have

$$Pr(r_{i+1} \mid r_i) = \text{Bin}(r_{i+1} - r_i \mid N - r_i, \tilde{z}_{i+1}). \quad (17)$$

The probability for $r_{i+1} = k \in I_{i+1}$ to occur in a scaled ECDF trajectory t_0^K which stayed within the simultaneous confidence bands until point i , that is, for which we have

$$t_0^i \in \bigcap_{j=0}^i T_j(\gamma), \quad (18)$$

can thus be written recursively as

$$Pr\left(r_{i+1} = k \cap \bigcap_{j=0}^i T_j(\gamma)\right) = \sum_{m \in I_i} Pr\left(r_i = m \cap \bigcap_{n=0}^{i-1} T_n(\gamma)\right) Pr(r_{i+1} = k \mid r_i = m). \quad (19)$$

The recursion is initialized at $z_0 = 0$ with $Pr(r_0 = 0) = 1$ so that $Pr(T_0(\gamma)) = 1$ for all $\gamma \in [0, 1]$. At any point $i \in \{0, \dots, K\}$, we can obtain

$$Pr\left(\bigcap_{j=0}^i T_j(\gamma)\right) = \sum_{m \in I_i} Pr\left(x_i = m \cap \bigcap_{n=0}^{i-1} T_n(\gamma)\right), \quad (20)$$

which is equal to $Pr(T(\gamma))$ when arriving at $i = K$. Clearly, $Pr(T(\gamma))$ is monotonically decreasing but not continuous in γ due to the discrete nature of the binomial distribution. Thus, Equation (15) will not have an exact solution in general and so we will not be able to meet the simultaneous confidence level $1 - \alpha$ exactly. We can, however, try to get as close as possible by computing

$$\hat{\gamma} = \arg \min_{\gamma \in [0, \alpha]} |1 - \alpha - Pr(T(\gamma))| \quad (21)$$

with a unidimensional derivative-free optimizer. In our experiments, the optimizer proposed by Brent (1973) (which is implemented, e.g., in the R function `optimize`) converged quickly in all cases to $\hat{\gamma}$ values implying a simultaneous confidence level very close to the nominal $1 - \alpha$.

3 Comparison of multiple samples

In this section, we extend the uniformity test of section 2 to test whether multiple samples originate from the same underlying distribution. In the case of multiple samples sharing the same distribution, the rank statistics of the values within each sample, when ranked jointly across all samples, are uniformly distributed on the interval $(1, \tilde{N})$, where \tilde{N} is the total length of the combined sample (Vehtari et al. 2021). Thus, instead of considering the sampled values directly, we consider the implied jointly rank-transformed values below.

3.1 Pointwise confidence bands

An important distinction to the ECDF case considered in section 2, is the form of the marginal distribution at quantile z_i when determining the adjusted coverage parameter γ . As our main application is the comparison of distributions induced by MCMC chains, we speak of the L different samples as chains and assume all chains to have the same

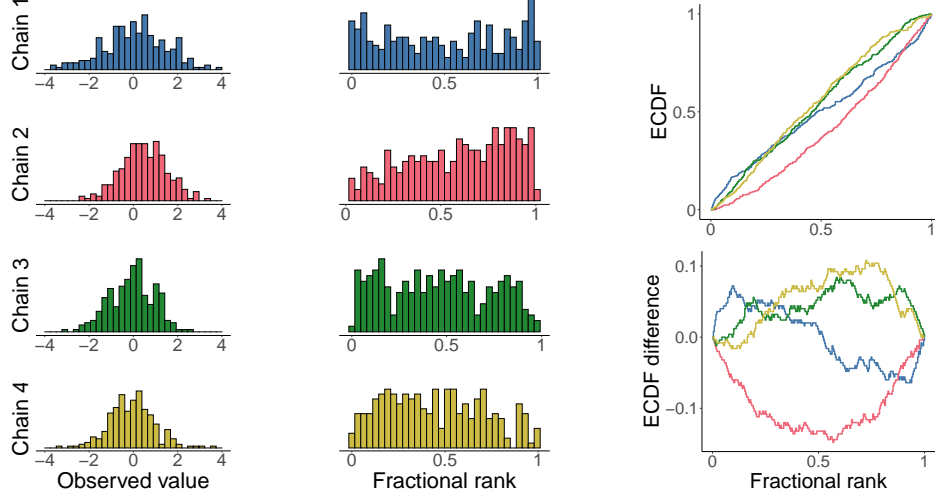


Figure 5: We evaluate the hypothesis of the four samples on the left originating from the same underlying distribution by inspecting the distribution of fractional ranks among the jointly rank transformed, Eq. (26), samples presented in the middle. When comparing multiple samples, we would like to take into account the within the sample dependency, but also the between sample dependency introduced by the joint transformation. In Sections 3.2 and 3.3 we extend our methods in order to provide simultaneous confidence bands for the ECDF and the ECDF difference plots shown on the right.

length N . We define r_i as the vector (of length L) of joint ranks across chains smaller than or equal to the sample size $s_i = \lfloor z_i N L \rfloor$. That is, for each of the L elements r_{il} of r_i , we have

$$r_{il} = \left\{ \sum_{j=1}^N \mathbb{I}_{\{1, \dots, s_i\}} (R(u_{lj} \mid u)) \right\}, \quad (22)$$

where u_{lj} is the j th draw of the l th chain before transformation, $R(u_{lj} \mid u)$ is the rank of u_{lj} within the vector u of all draws across all chains, and \mathbb{I} is the indicator function. Clearly, because of the definition of ranks, we know for all i that

$$\sum_{l=1}^L r_{il} = s_i, \quad (23)$$

and we define the set of all r_i satisfying (23) as R_i . Due to the pairwise independence of the original draws u_{lj} (by assumption), the marginal distribution of r_i at quantile z_i is multivariate hypergeometric

$$r_i \sim \text{MHyp}(\tilde{N}, s_i), \quad (24)$$

where $\tilde{N} = (N_1, \dots, N_L)$ is the vector chain lengths (i.e., population sizes) and $N_1 = \dots = N_L = N$ as we assume chains to have equal length. It is well known that, in this case, the marginal distribution of r_{il} , and thus the distribution defining the pointwise confidence bands, is hypergeometric

$$r_{il} \sim \text{Hyp}(N, N(L-1), s_i). \quad (25)$$

3.2 Simultaneous confidence bands through simulation

In this section, we extend the simulation method presented in Section 2.2 to comparison of multiple samples. Our aim is to define simultaneous confidence bands for the ECDFs of multiple, jointly rank-transformed distributions so that the interior of the simultaneous confidence bands jointly contains all trajectories induced by the rank-transformed distributions with rate $1 - \alpha$. To this end, we define r_i and s_i as in Section 3.1 and denote the interior of the simultaneous confidence bands at quantile z_i as $\tilde{I}_i(\gamma)$, with γ being the adjusted coverage parameter to be determined.

We continue the use of fractional ranks in the ECDF plots to provide illustrations independent of the length of the sampled chains. Suppose we have L chains of length N . The fractional rank score \tilde{r}_{il} corresponding to the i th value of the l th chain, u_{li} , is

$$\tilde{r}_{il} = \frac{R(u_{li} \mid u)}{LN}. \quad (26)$$

Instead of using the adjusted value of γ to obtain the $1 - \alpha$ level simultaneous confidence bands for a single ECDF trajectory, we adjust γ to account for the dependence between the samples introduced in the transformation into fractional ranks. That is, after choosing the evaluation quantiles z_i , we adjust γ to find upper and lower simultaneous confidence bands satisfying

$$\Pr(L_i(\gamma) \leq F_l(z_i) \leq U_i(\gamma) \mid \forall i, l) = 1 - \alpha, \quad (27)$$

where F_l is the ECDF of the fractional rank scores of the l th chain.

We denote the CDF of the hypergeometric distribution as Hyp and its inverse as Hyp^{-1} . The algorithm to approximate the adjusted coverage parameter γ when comparing L samples is as follows:

1. For $m = 1, \dots, M$:

- (a) Simulate $u_{11}^m, \dots, u_{LN}^m \sim \text{uniform}(0, 1)$, $l = 1, \dots, L$.
- (b) For $j = 1, \dots, N$ and $l = 1, \dots, L$, compute \tilde{r}_{jl}^m .
- (c) For $i = 1, \dots, K$ and $l = 1, \dots, L$, compute $F_l^m(z_i)$.
- (d) For $i = 1, \dots, K$ and $l = 1, \dots, L$, compute

$$\text{Hyp}(NF_l^m(z_i) \mid N, (L-1)N, s_i) \text{ and } \text{Hyp}(NF_l^m(z_i) - 1 \mid N, (L-1)N, s_i),$$

where $s_i = \lfloor z_i NL \rfloor$.

- (e) Find the minimum probability

$$\gamma^m = 2 \min_{i,l} \{ \min(\text{Hyp}(NF_l^m(z_i) \mid N, (L-1)N, s_i), 1 - \text{Hyp}(NF_l^m(z_i) - 1 \mid N, (L-1)N, s_i)) \}.$$

2. Set γ to be the 100α percentile of $\{\gamma^1, \dots, \gamma^M\}$.

3. Form the confidence bands

$$[L_i(\gamma), U_i(\gamma)] = \left[\text{Hyp}^{-1}\left(\frac{\gamma}{2} \mid N, N(L-1), s_i\right), \text{Hyp}^{-1}\left(1 - \frac{\gamma}{2} \mid N, N(L-1), s_i\right) \right],$$

for $i = 1, \dots, K$.

3.3 Simultaneous confidence bands through optimization

In this section, we extend the optimization method presented in Section 2.3 to comparison of multiple samples. With the marginal distribution of r_{il} being hypergeometric, the rank interior $I_i(\gamma)$ for x_i is given by

$$I_i(\gamma) = \left\{ r \in R_i \mid \forall r_l \in r : \text{Hyp}^{-1}\left(\frac{\gamma}{2} \mid N, N(L-1), s_i\right) \leq r_l \leq \text{Hyp}^{-1}\left(1 - \frac{\gamma}{2} \mid N, N(L-1), s_i\right) \right\}. \quad (28)$$

We treat the borders between interior and exterior as belonging to the interior. Based on $I_i(\gamma)$, we can again easily obtain $\tilde{I}_i(\gamma)$, as $r \in I_i(\gamma)$ is equivalent to $r/N \in \tilde{I}_i(\gamma)$.

The remainder of the proof proceeds similar to the one-sample case except that we replace the binomial distribution with the (multivariate) hypergeometric distribution. A (multivariate) rank ECDF trajectory defined as

$$t_0^K = ((z_i)_{i=0}^K, (r_i)_{i=0}^K), \quad (29)$$

where $z_0 = 0$ and $z_K = 1$, stays within the simultaneous confidence bands completely if and only if $r_i \in I_i(\gamma)$ for all $i \in \{0, \dots, K\}$. If we denote the set of trajectories fulfilling $r_i \in I_i$ as T_i , we can write the set of trajectories which are completely in the interior of the simultaneous confidence bands as

$$T(\gamma) = \bigcap_{i=0}^K T_i(\gamma). \quad (30)$$

In order for the simultaneous confidence bands to have a confidence level $1 - \alpha$, we must satisfy

$$\Pr(T(\gamma)) = 1 - \alpha. \quad (31)$$

Due to the pairwise independence of the original draws u_{ij} (by assumption), the distribution of the rank ECDF trajectories is Markovian. That is, any ECDF trajectory t_{i+1}^K beyond a given point (z_i, r_i) only depends on (z_i, r_i) but not on the history of how we got there. This implies that, under the assumption of all chains coming from the same underlying distribution, the growth $r_{i+1} - r_i$ of the ECDF from z_i to z_{i+1} is multivariate hypergeometric with $\tilde{N}_i = \tilde{N} - r_i$ and sample size $\tilde{s}_{i+1} = s_{i+1} - s_i$. Accordingly, we have

$$\Pr(r_{i+1} \mid r_i) = p_{\text{MHYP}}(r_{i+1} - r_i \mid \tilde{N}_i, \tilde{s}_{i+1}), \quad (32)$$

where p_{MHYP} denotes the discrete PDF of the multivariate hypergeometric distribution. The probability for $r_{i+1} = k \in I_{i+1}$ to occur in a rank ECDF trajectory t_0^K which stayed in the simultaneous confidence bands until point i , that is, for which we have

$$t_0^i \in \bigcap_{j=0}^i T_j(\gamma) \quad (33)$$

can thus be written recursively as

$$\Pr\left(r_{i+1} = k \cap \bigcap_{j=0}^i T_j(\gamma)\right) = \sum_{m \in I_i} \Pr\left(r_i = m \cap \bigcap_{n=0}^{i-1} T_n(\gamma)\right) \Pr(r_{i+1} = k \mid r_i = m). \quad (34)$$

The recursion is initialized at $z_0 = 0$ with $\Pr(x_0 = (0, \dots, 0)) = 1$ so that $\Pr(T_0(\gamma)) = 1$ for all $\gamma \in [0, 1]$. At any point $i \in \{0, \dots, K\}$, we can obtain

$$\Pr\left(\bigcap_{j=0}^i T_j(\gamma)\right) = \sum_{m \in I_i} \Pr\left(r_i = m \cap \bigcap_{n=0}^{i-1} T_n(\gamma)\right), \quad (35)$$

which is equal to $\Pr(T(\gamma))$ when arriving at $i = K$. Clearly, $\Pr(T(\gamma))$ is monotonically decreasing but not continuous in γ due to the discrete nature of the (multivariate) hypergeometric distribution. We can compute

$$\hat{\gamma} = \arg \min_{\gamma \in [0, \alpha]} |1 - \alpha - \Pr(T(\gamma))| \quad (36)$$

using a unidimensional derivative-free optimizer. In our experiments, the optimizer proposed by Brent (1973) converged in all cases to $\hat{\gamma}$ values implying a simultaneous confidence level very close to the nominal $1 - \alpha$.

Unfortunately, evaluating Eq. (34) suffers from combinatorial explosion as the R_i are L -dimensional sets constraint only by Equation (23) and as $\Pr(r_{i+1} = k \mid r_i = m)$ has to be computed for all combinations of elements $k \in I_{i+1}$ and $m \in I_{i+1}$ at each point i . Several measures can be taken to reduce the complexity of the computation. First, the ranks of one of the L chains are redundant as they follow deterministically from Equation (23) based on the ranks of the other $L - 1$ chains. This implies in particular that the 2-chain case has the same computational complexity as the one-sample case as only one of the two chains needs to be evaluated. Second, due to a-priori symmetry of the chains, we can, without loss of generality, assume at the first non-zero quantile z_1 that the elements r_{1l} of r_1 are ordered such that $r_{11} \leq r_{12} \leq \dots \leq r_{1L}$. This reduces the number of trajectories to be evaluated by a factor of $L(L + 1)/2$. Still even with these measures in place, computation will scale badly with L , and simulation based method or grid-based interpolation of pre-computed values is faster for larger number of chains.

4 Numerical Experiments and Power Analysis

In this section, we provide insights into how the plots produced by our proposed methods should be interpreted. In each of the following cases, we link together the histogram, ECDF plot, and the ECDF difference plot. The code for the experiments and plots is available at <https://github.com/TeemuSailynoja/simultaneous-confidence-bands>.

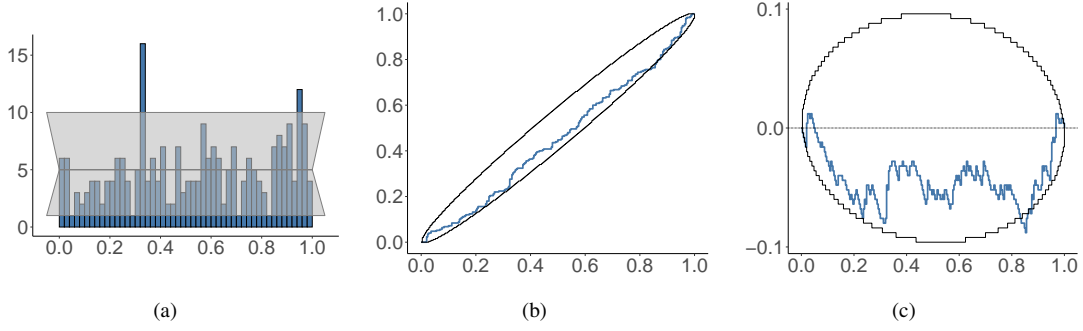


Figure 6: Effect of difference in sample mean. (a) Histogram with 50 uniformly spaced bins, (b) ECDF plot, and (c) ECDF difference plot of the fractional ranks of a sample of 250 values with larger than expected mean. In the histogram, 95% confidence intervals are provided for each bin, in plots (b) and (c) 95% simultaneous confidence bands are provided for the ECDF.

4.1 Uniformity of a Single Sample

We begin by providing two examples connecting the shape of the histogram of the transformed sample to the characteristics of the corresponding ECDF and ECDF difference plots with basic discrepancies between the sample and the comparison distribution. After this we illustrate an application of our method as part of a workflow to detect issues in model implementation or the computation of the posterior distribution. Lastly we provide power analysis comparing the performance of our proposed method to existing state of the art tests for uniformity.

With the exception of the power analysis tests in 4.1.4 where the samples are drawn directly from a continuous uniform distribution, the samples in the following examples are transformed to the unit interval from their respective sampling distributions through empirical PIT and are tested against the hypothesis of discrete uniformity.

4.1.1 Effect of Difference in Sample Mean

To observe the typical characteristics of a sample with a mean different than that of the comparison distribution, we draw $y = y_1, \dots, y_N \sim \text{normal}(0.3, 1)$ and a comparison sample $x = x_1, \dots, x_N \sim \text{normal}(0, 1)$ with $N = 250$. We then test for y being standard normal distributed by transforming the samples values to the unit interval with the empirical PIT. Figure 6(a) shows the histogram of the transformed sample exhibiting a higher than expected mean. As seen in the figure, a shift in the sample mean leads to the histogram being slanted towards the direction of the shift. The ECDF plot in Figure 6(b), shows this shift through the ECDF graph remaining under the theoretical CDF, which is also seen in the ECDF difference plot in Figure 6(c). If the sample in question would instead have a mean lower than expected, the histogram would be slanted to the left and the behaviour of the resulting ECDF plot and ECDF difference plot would be reversed. That is, the ECDF plot would stay above the theoretical CDF as a higher than expected density is covered at low fractional ranks and the ECDF difference plot would respectively show a \cap -shape above the zero level.

4.1.2 Effect of Difference in Sample Variance

Next, we investigate an example where the sample has a higher than expected variance. To this end we draw $y = y_1, \dots, y_N \sim \text{normal}(0, 1.3)$ and a standard uniform comparison sample $x = x_1, \dots, x_N \sim \text{normal}(0, 1)$ with $N = 250$. Figure 7(a) shows the histogram of the empirical PIT values. In general, a larger than expected variance leads to a U-shaped histogram and one can indeed see some of the histogram bins breaching the 95% confidence bounds. In the ECDF plot shown in Figure 7(b), the larger than expected variance leads to faster than expected growth near the edges and slower than expected growth in the middle. The shape is more clearly seen in the ECDF difference plot in Figure 7(c) depicting the difference between the ECDF and the theoretical CDF. If the sample would instead present a variance lower than expected, the histogram would be \cap -shaped and the behaviour of the resulting ECDF plot and ECDF difference plot would be reversed. In the ECDF plot this is shown as faster increase near the middle. In general, the ECDF difference plot is decreasing when a smaller than expected density of samples is covered, and correspondingly increases when covering a higher than expected density.

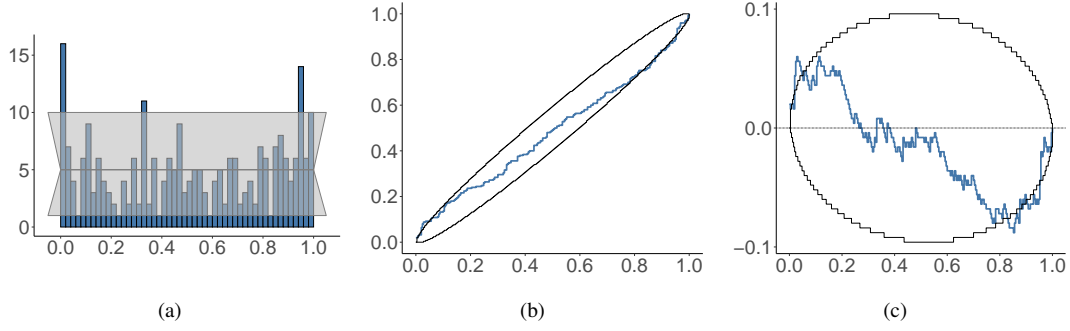


Figure 7: Effect of difference in sample variance. (a) Histogram with 50 uniformly spaced bins, (b) ECDF plot, and (c) ECDF difference plot of the fractional ranks for a sample of 250 values with larger than expected variance. In the histogram, 95% confidence intervals are provided for each bin, in the two plots depicting the ECDF, 95% simultaneous confidence bands are provided.

4.1.3 Simulation Based Calibration: Eight Schools

The eight schools (Gelman, Carlin, et al. 2013), is a classic hierarchical model example. The training course effects θ_j in eight schools are modelled using an hierarchical varying intercept model.

If the model is constructed with the centered parameterization, the posterior distribution exhibits a funnel shape contracting to a region of high curvature near the population mean μ when sampled with small values of the population standard deviation τ . This property makes exploring the distribution of τ difficult for many MCMC methods. The centered parameterization $(\theta, \mu, \tau, \sigma)$ of the problem is as follows:

$$\theta_j \sim \text{normal}(\mu, \tau) \quad (37)$$

$$y_j \sim \text{normal}(\theta_j, \sigma_j). \quad (38)$$

As explained by Talts et al. (2020), when we consider a sample drawn from the Bayesian joint distribution and the resulting posteriors,

$$\tilde{u} \sim \pi(u) \quad (39)$$

$$\tilde{y} \sim \pi(y \mid \tilde{u}) \quad (40)$$

$$\{u_1, \dots, u_L\} \sim \pi(u \mid \tilde{y}), \quad (41)$$

the rank statistic of the prior sample \tilde{u} in relation to the posterior draws $\{u_1, \dots, u_L\}$ should be uniformly distributed.

When using simulation-based calibration (SBC) as proposed by Talts et al. (2020), one looks for deviations from uniform in the resulting rank distributions as these suggest either issues in the posterior computation or in the model implementation. As seen from Figure 8, the prior draws of the population standard deviation τ ranked in relation to the posterior samples obtained from the centered parameterization of the eight schools model are skewed to large ranks, suggesting the MCMC is not sampling correctly from the target distribution (which in this case is known to be caused by inability to reach the narrow funnel part of the posterior).

In Section 4.2.4, we will return to the eight schools model by providing further analysis on the convergence of individual chains in the centered parameterization case and illustrating how our method can be used to detect these convergence issues.

4.1.4 Power analysis

To compare our method with existing tests for uniformity, we consider the rejection rate of samples drawn from uniform distribution and then transformed according to the following three transformation families Marhuenda, Morales, and

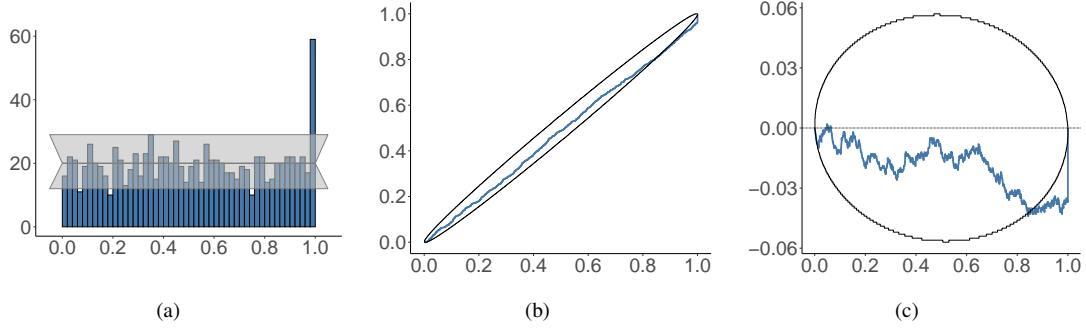


Figure 8: (a) Histogram, (b) ECDF plot, and (c) ECDF difference plot of prior draw ranks of the parameter τ in the centered parameterization eight schools model.

Pardo (2005) use in their article comparing various tests for uniformity:

$$f_{A,k}(x) = 1 - (1 - x)^k, \quad 0 \leq x \leq 1, \quad (42)$$

$$f_{B,k}(x) = \begin{cases} 2^{k-1}x^k & \text{if } 0 \leq x \leq 0.5 \\ 1 - 2^{k-1}(1 - x)^k & \text{if } 0.5 < x \leq 1 \end{cases} \quad (43)$$

$$f_{C,k}(x) = \begin{cases} 0.5 - 2^{k-1}(0.5 - x)^k & \text{if } 0 \leq x \leq 0.5 \\ 0.5 + 2^{k-1}(x - 0.5)^k & \text{if } 0.5 < x \leq 1. \end{cases} \quad (44)$$

As Marhuenda, Morales, and Pardo (2005) offer an extensive comparison of tests, we limit our comparison to the test recommended for each of the transformation families in addition to the widely known Kolmogorov-Smirnov test. For each of the test statistics, a critical value is calculated and samples exceeding that value are rejected.

For transformation family A, the recommended test is the mean distance of the i th value of the ordered sample $u_{(i)}$ from the expected value $i/(N + 1)$:

$$T_1 = \sum_{i=1}^N \frac{|u_{(i)} - i/(N + 1)|}{N}. \quad (45)$$

For family B, the smooth goodness-of-fit test, N_h , introduced by Neyman (1937) is recommended with the dimension h chosen according to the method recommended by Ledwina (1994) resulting in the test statistic N_S , which also has the best overall performance across the transformation families. The test recommended for transformation family C is the statistic recommended by Watson (1961),

$$U^2 = W^2 - i(\bar{u} - 0.5)^2, \quad (46)$$

where \bar{u} is the mean of the u_i and W^2 is the Cramér-von Mises statistic,

$$W^2 = \sum_{i=1}^N \left\{ u_{(i)} - \frac{2i - 1}{2N} \right\}^2 + \frac{1}{12N}. \quad (47)$$

The rejection rates of these tests and our ECDF simultaneous confidence bands are shown in Figure 9 for families A, B, and C with sample size $N = 100$ and k varying between 0.20 and 3.00. For each value of k , the rejection rate among 100,000 samples was computed. As seen from these results, the proposed ECDF simultaneous confidence band method performs in a manner similar to the recommended tests with the exception to family C, where our method exhibits a lower rejection rate compared to some of the other tests.

4.2 Comparing Multiple Samples

When testing if two or more samples are produced from the same underlying distribution, we can compare the ranks of each sample relative to the sample obtained by combining all the samples in the comparison. As mentioned in Section 3, we need to adjust the confidence bands to take into account the dependency of the ranks of the values of one sample on the values in other samples in the comparison.

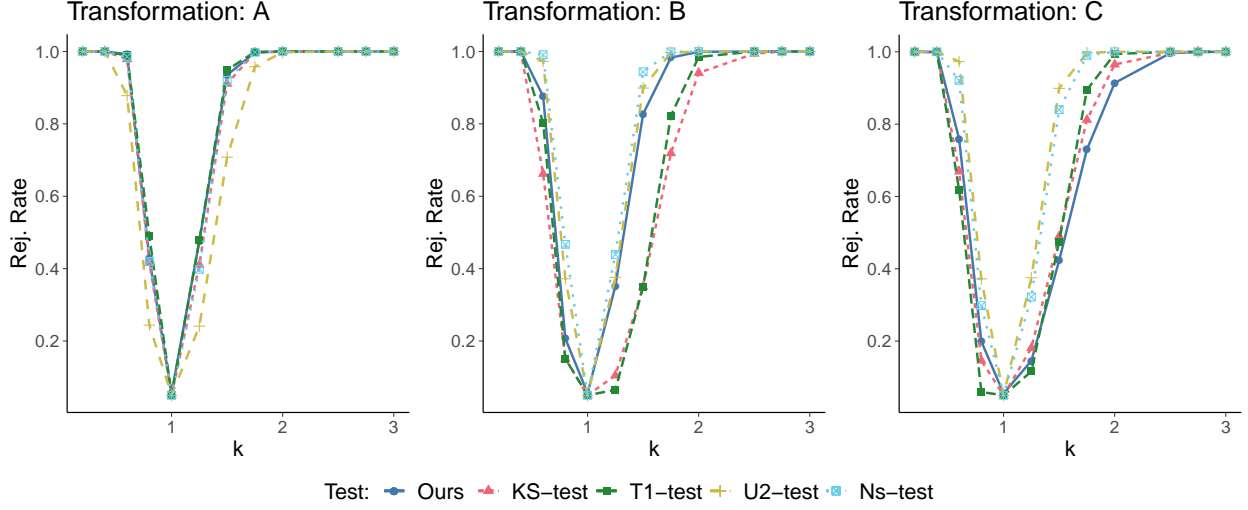


Figure 9: Comparison of uniformity test powers between existing tests and the graphical confidence band test for three families of deviations from the uniform distribution.

4.2.1 Effect of difference in means and variances

We first compare two cases of MCMC sampling with four chains. In each case, chains 2 to 4 were sampled from a $\text{normal}(0, 1)$ distribution. In the first case, chain 1 is sampled with a larger mean than the other chains, $\text{normal}(0.5, 1)$. In the second case, chain 1 is sampled with a larger variance, $\text{normal}(0, 1.5)$.

Rank plots for the first case with larger mean in one chain are shown in Figure 10(a)-(d). Even though the difference in the sampling distribution of chain 1 can be seen in the histograms with 50 bins, this effect is more clearly represented in the ECDF difference plot in Figure 10(f) where chain 1 shows the shape familiar from 4.1.1 and chains 2 to 4 show a reverse shape, indicating similar behaviour between these three chains. Similar remarks regarding the behaviour of the chains can be made from the ECDF plot in Figure 10(e), but the more dynamic range of the ECDF difference plot in Figure 10(f) makes the difference in the behaviour of the chains clearer. In the second case, where chain 1 is sampled with a higher variance, we can see a U-shape in the rank plot of chain 1 in Figure 11(a), but the behaviour stands out more clearly in the ECDF difference plot in Figure 11(f).

4.2.2 Test performance under common deviations

To evaluate the performance of the multiple sample comparison test under a set of common deviations, one of the samples was transformed according to the three transformation families defined in equation (42). In the analysis 2, 4, and 8 chains of length 100 were simulated from $U(0, 1)$ after which one of the chains was transformed according to the transformations $f_{A,k}$, $f_{B,k}$, and $f_{C,k}$. The rejection rates of the multiple sample comparison test when varying the power, k , of the transformation were estimated from 10,000 simulations and are recorded in Figure 12. The observed test performance is independent of the number of chains used in the sample comparison. When compared to the rejection rates observed in the single sample power analysis in 4.1.4, the rejection rates show that the test sensitivity depends in a similar way on the transformation.

4.2.3 Chains with autocorrelation

As samples generated by MCMC processes are typically autocorrelated, it is essential to analyse the performance of the sample comparison test under autocorrelated samples. In Figure 13, rejection rates of simulated multiple sample test 2, 4, and 8 chains produced by autoregressive models of order 1 (i.e., AR(1) models) with varying AR-parameter values are presented. Each rejection rate is computed as the mean of 100,000 simulations. As seen in the figure, the higher the autocorrelation in the samples is and the more chains are sampled, the more likely the test is to reject the hypothesis that the samples are drawn from the same underlying distribution. Thus, before using the graphical illustration or the

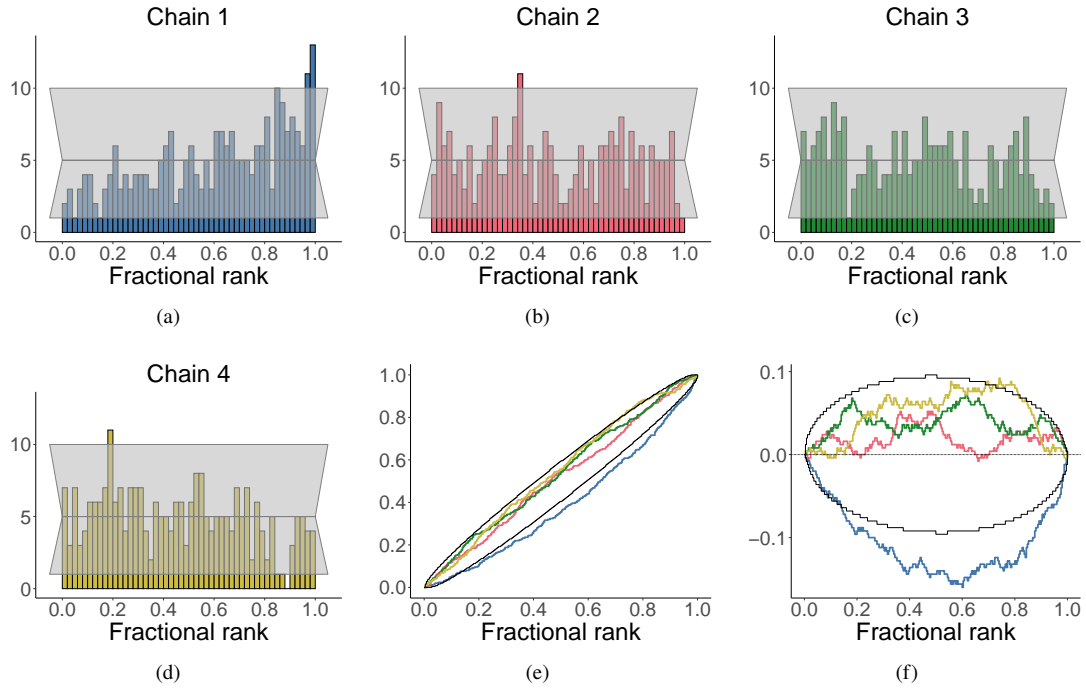


Figure 10: Effect of differences in means. (a)-(d) Rank plots, (e) ECDF plot, and (f) ECDF difference plot of four chains with chain 1 sampled with a larger mean.

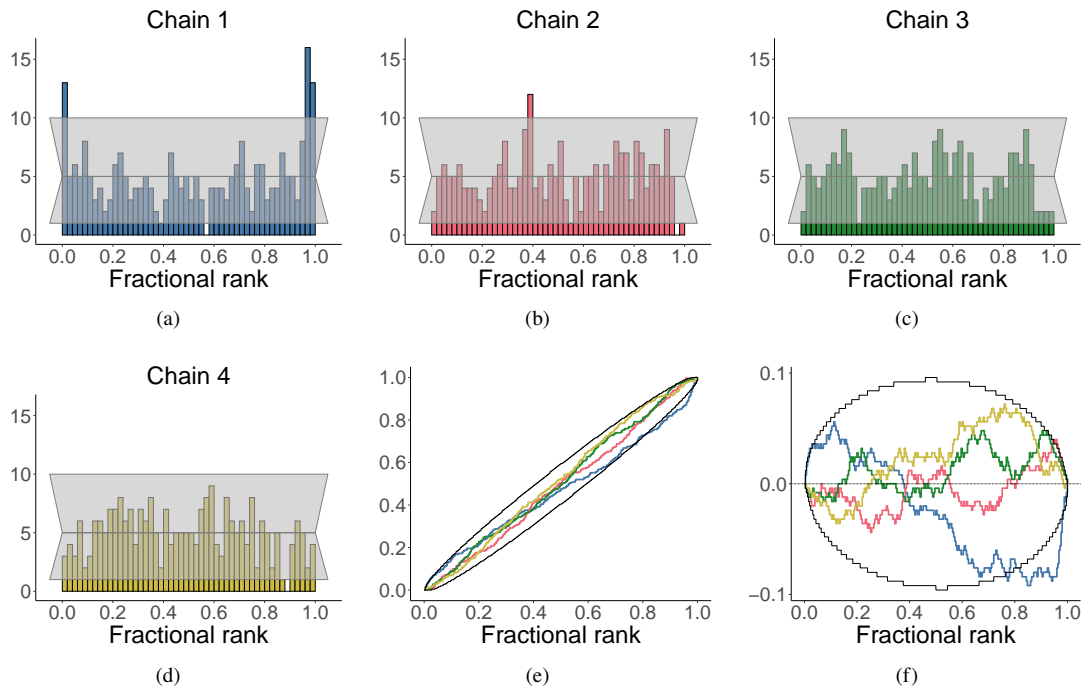


Figure 11: Effect of difference in variances. (a)-(d) Rank plots, (e) ECDF plot, and (f) ECDF difference plot of four chains with chain 1 sampled with a larger variance.

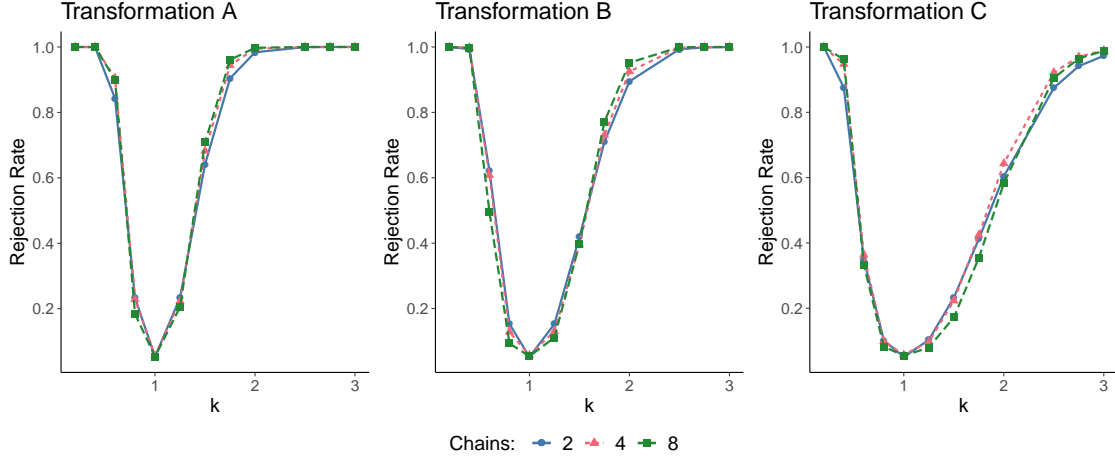


Figure 12: Analysis of sample comparison test powers when one of the chains is transformed according to one of the three transformation families.

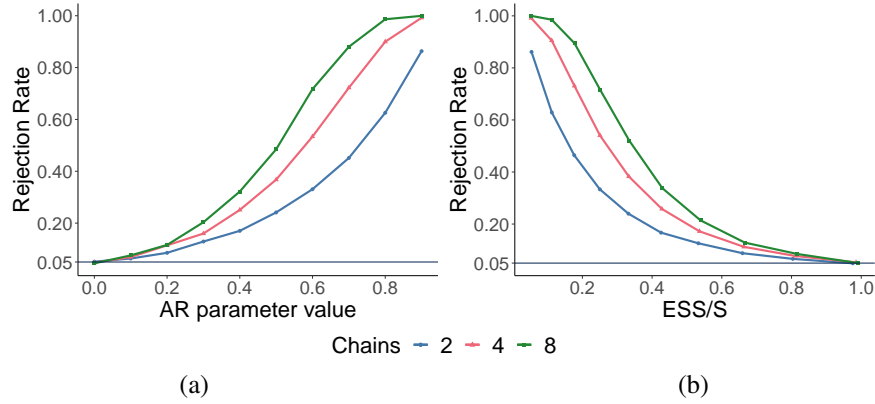


Figure 13: Test rejection rate when comparing chains with autocorrelation. In (a) as a function of the AR-parameter value. In (b) as a function of the ratio between effective sample size and the total sample size. The nominal rejection rate 0.05 is shown with a vertical line in both plots.

corresponding test, the chains should be thinned to have negligible autocorrelation. The same holds for other common uniformity tests as well, as they rely on the assumption of pairwise independence of draws.

4.2.4 Detecting model sampling issues: eight schools

We return to the eight schools model used to demonstrate SBC in Section 4.1.3. The issues detected with SBC earlier are apparent when we use multiple sample comparison to inspect the rank distribution between the individual chains. Even when sampled with more conservative settings of the sampler, we see from Figure 14 that the chains are not properly exploring the posterior and thus the realized rank transformed chains have clearly different ECDFs.

As recommended in Section 22.7 of the Stan User's Guide (Stan Development Team 2020), these observed sampling issues of a hierarchical model with weak likelihood contribution can often be avoided by using the non-centered parameterization $(\tilde{\theta}, \mu, \tau, \sigma)$ of the model:

$$\tilde{\theta}_j \sim \text{normal}(0, 1) \quad (48)$$

$$\theta_j = \mu + \tau \tilde{\theta}_j \quad (49)$$

$$y_j \sim \text{normal}(\theta_j, \sigma_j) \quad (50)$$

In the above parameterization, the treatment effect θ_j is derived deterministically from the other parameter values

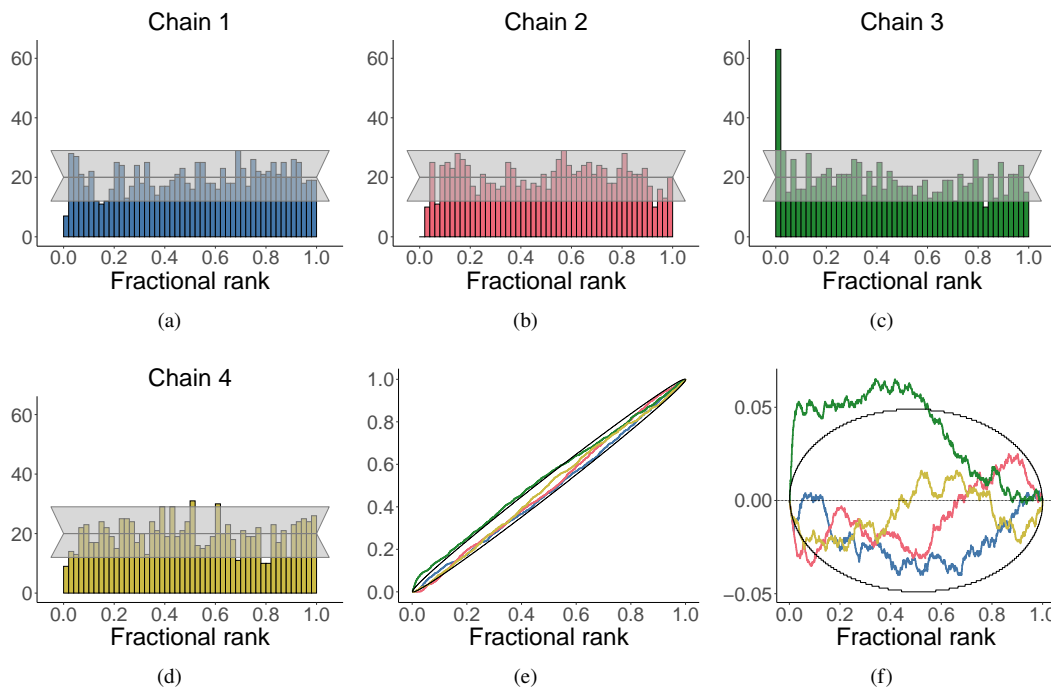


Figure 14: Detecting model sampling issues. Rank plots (a)-(d), (e) ECDF and (f) ECDF difference plot of posterior draws from four chains for the centered parameter eight schools model.

and instead $\tilde{\theta}_j$ is sampled. To keep the models comparable, we use the same conservative sampling options for the non-centered model although this is not required to obtain well mixing chains. In Figure 15, we see an improvement in the sampling compared to the centered parameterization, as the sample ranks are distributed approximately uniformly among the four chains implying that the chains are mixing well.

5 Discussion

By providing a graphical test for uniformity and comparison of samples, we offer an accessible tool to be used in many parts of practical statistical workflow.

For assessing the uniformity of a single sample, we recommend the optimization-based adjustment method, as it is efficient even for large sample sizes. For comparing multiple samples, the simulation-based method is likely to be computationally more efficient than the optimization-based method. To speed-up the computations, we recommend to pre-compute adjusted γ values for a set of sample size and number of samples (chains) and then interpolate (in log-log space) the adjustment as needed.

In the examples we used empirical PIT with SBC, where the uniformity is expected by construction if the inference algorithm works correctly. PIT has also been used to compare predictive distributions. Specifically, in the LOO-PIT approach, PIT has been used to compare leave-one-out (LOO) cross-validation predictive distributions to the observations (e.g. Gneiting, Balabdaoui, and Raftery 2007; Czado, Gneiting, and Held 2009). Although the graphical LOO-PIT test is useful for visualization of model-data discrepancy, exact uniformity of LOO-PIT values can be expected only asymptotically given the true model. For example, if the data comes from a normal distribution and is modeled with a normal distribution with unknown mean and scale, the posterior predictive distribution is a Student's t distribution that approaches normal only asymptotically. Thus use of graphical LOO-PIT tests needs further research.

We have assumed that distributions g and p are continuous and only the fractional rank statistics u_i from Eq. (2) are discrete. Our proposed methods do not work directly if g and p are discrete, as values obtained through PIT are no longer uniform. Also, in the multiple sample comparison case, the rank statistics are no longer mutually distinct as ties are possible. The potential approach to handling discrete g and p is to use randomized or non-randomized modifications

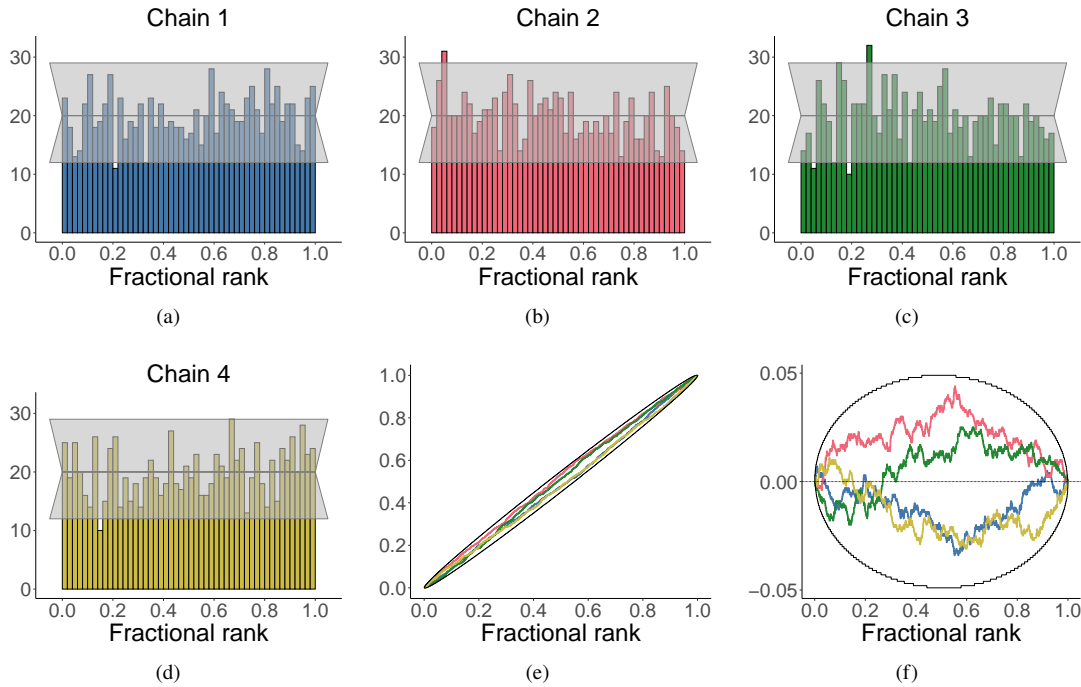


Figure 15: Detecting model sampling issues. (a)-(d) Rank plots, (e) ECDF and (f) ECDF difference plot of posterior draws from four chains for the non-centered parameter eight schools model.

of PIT values for discrete distributions as discussed by Czado, Gneiting, and Held (2009). However, developing proven and efficient algorithms for this purpose requires further work which is left for future research.

Acknowledgments

We thank the Academy of Finland (grant 298742), the Finnish Center for Artificial Intelligence, and the Technology Industries of Finland Centennial Foundation (grant 70007503; Artificial Intelligence for Research and Development) for partial support of this research. We also acknowledge the computational resources provided by the Aalto Science-IT project.

References

- Aldor-Noiman, Sivan et al. (2013). “The Power to See: A New Graphical Test of Normality”. In: *The American Statistician* 67.4, pp. 249–260. DOI: [10.1080/00031305.2013.847865](https://doi.org/10.1080/00031305.2013.847865).
- Arnold, Barry C., N. Balakrishnan, and H. N. Nagaraja (2008). *A First Course in Order Statistics (Classics in Applied Mathematics)*. USA: Society for Industrial and Applied Mathematics. ISBN: 0898716489.
- Brent, RP (1973). “An algorithm with guaranteed convergence for finding the minimum of a function of one variable”. In: *Algorithms for Minimization without Derivatives, Prentice-Hall, Englewood Cliffs, NJ*, pp. 61–80.
- Czado, Claudia, Tilmann Gneiting, and Leonhard Held (2009). “Predictive Model Assessment for Count Data”. In: *Biometrics* 65.4, pp. 1254–1261.
- D’Agostino, Ralph B and Michael A Stephens (1986). *Goodness-of-Fit Techniques*. USA: Marcel Dekker, Inc. ISBN: 0824774876.
- Gelman, Andrew, John B Carlin, et al. (2013). *Bayesian data analysis*. 3rd ed. CRC press.
- Gelman, Andrew, Aki Vehtari, et al. (2020). “Bayesian Workflow”. In: *arXiv preprint arXiv:2011.01808*.
- Gneiting, Tilmann, Fadoua Balabdaoui, and Adrian E Raftery (2007). “Probabilistic forecasts, calibration and sharpness”. In: *Journal of the Royal Statistical Society: Series B* 69.2, pp. 243–268.

- Kolmogorov, Andrey (1933). “Sulla determinazione empirica di una legge di distribuzione”. In: *Inst. Ital. Attuari, Giorn.* 4, pp. 83–91.
- Ledwina, Teresa (Sept. 1994). “Data-Driven Version of Neyman’s Smooth Test of Fit”. In: *Journal of the American Statistical Association* 89.427, pp. 1000–1005. DOI: [10.1080/01621459.1994.10476834](https://doi.org/10.1080/01621459.1994.10476834).
- Marhuenda, Y., D. Morales, and M. C. Pardo (Aug. 2005). “A comparison of uniformity tests”. In: *Statistics* 39.4, pp. 315–327. DOI: [10.1080/02331880500178562](https://doi.org/10.1080/02331880500178562).
- Massey Jr, Frank J (1951). “The Kolmogorov-Smirnov test for goodness of fit”. In: *Journal of the American statistical Association* 46.253, pp. 68–78.
- Neyman, J. (July 1937). “»Smooth test» for goodness of fit”. In: *Scandinavian Actuarial Journal* 1937.3-4, pp. 149–199. DOI: [10.1080/03461238.1937.10404821](https://doi.org/10.1080/03461238.1937.10404821).
- Stan Development Team (2020). *Stan User’s Guide*. URL: https://mc-stan.org/docs/2_24/stan-users-guide/index.html (visited on 09/29/2020).
- Talts, Sean et al. (2020). “Validating Bayesian inference algorithms with simulation-based calibration”. In: *arXiv preprint arXiv:1804.06788v2*.
- Vehtari, Aki et al. (2021). “Rank-normalization, folding, and localization: An improved \hat{R} for assessing convergence of MCMC”. In: *Bayesian analysis*. DOI: [10.1214/20-BA1221](https://doi.org/10.1214/20-BA1221).
- Watson, G. S. (1961). “Goodness-of-fit tests on a circle”. In: *Biometrika* 48.1-2, pp. 109–114. DOI: [10.1093/biomet/48.1-2.109](https://doi.org/10.1093/biomet/48.1-2.109).